

Metabolic engineering of *Pseudomonas taiwanensis* VLB120 for rhamnolipid biosynthesis from biomass-derived aromatics

Vaishnavi Sivapuratharasan^{a,b}, Christoph Lenzen^a, Carina Michel^a,
Anantha Barathi Muthukrishnan^b, Guhan Jayaraman^b, Lars M. Blank^{a,*}

^a Institute of Applied Microbiology, RWTH Aachen University, Worringerweg 1, 52074, Aachen, Germany

^b Department of Biotechnology, Bhupat and Jyoti Mehta School of Biosciences, Indian Institute of Technology Madras, Chennai, 600036, India

ARTICLE INFO

Keywords:

Biomass-derived aromatics
Aromatics degradation
Pseudomonas
Adaptive laboratory evolution
Metabolic engineering
Rhamnolipids

ABSTRACT

Lignin is a ubiquitously available and sustainable feedstock that is underused as its depolymerization yields a range of aromatic monomers that are challenging substrates for microbes. In this study, we investigated the growth of *Pseudomonas taiwanensis* VLB120 on biomass-derived aromatics, namely, 4-coumarate, ferulate, 4-hydroxybenzoate, and vanillate. The wild type strain was not able to grow on 4-coumarate and ferulate. After integration of catabolic genes for breakdown of 4-coumarate and ferulate, the metabolically engineered strain was able to grow on these aromatics. Further, the specific growth rate of the strain was enhanced up to 3-fold using adaptive laboratory evolution, resulting in increased tolerance towards 4-coumarate and ferulate. Whole-genome sequencing highlighted several different mutations mainly in two genes. The first gene was *actP*, coding for a cation/acetate symporter, and the other gene was *paaA* coding for a phenyl acetyl-CoA oxygenase. The evolved strain was further engineered for rhamnolipid production. Among the biomass-derived aromatics investigated, 4-coumarate and ferulate were promising substrates for product synthesis. With 4-coumarate as the sole carbon source, a yield of 0.27 (Cmol_{rh}/Cmol_{4-coumarate}) was achieved, corresponding to 28% of the theoretical yield. Ferulate enabled a yield of about 0.22 (Cmol_{rh}/Cmol_{ferulate}), representing 42% of the theoretical yield. Overall, this study demonstrates the use of biomass-derived aromatics as novel carbon sources for rhamnolipid biosynthesis.

1. Introduction

Lignin accounts for a substantial amount (15–30%) of lignocellulosic biomass that is abundantly found in our environment. However, lignin is under-utilized due to its high recalcitrance and heterogeneity. Currently, in biorefineries, lignin valorization is just limited to produce heat and electricity. Alternatively, lignin could be depolymerized to generate a range of aromatic monomers, which can be utilized as a substrate for manufacturing bio-based products. Different types of biomass-derived aromatics are generated during hydrolysis depending on the lignin used (Raj et al., 2007; Zhu et al., 2017). These aromatics can act as inhibitors for the growth of the commonly used industrial workhorses *Saccharomyces cerevisiae* and *Escherichia coli* (Adeboye et al., 2014; Palmqvist, 2000). There is a lack of metabolic pathways in some organisms to utilize aromatics. Therefore, there is an increasing need for research on the development of microbial hosts that can tolerate and utilize the aromatics as substrates and produce valuable products

(Becker and Wittmann, 2019). Various studies have reported deploying aromatics as substrates for different microbial hosts. *Acinetobacter baylyi* ADP1 was used to produce alkanes and wax esters (Salmela et al., 2019). With *S. cerevisiae*, protocatechuic acid was produced (Zhang et al., 2021), and also different *Pseudomonas* spp. were used for the formation of various industrially essential products such as itaconic acid (Elmore et al., 2021), muconic acid (Barton et al., 2018), adipic acid (van Duuren et al., 2020), polyhydroxyalkanoates (Borrero-de Acuña et al., 2021), 2-pyrone 4,6-dicarboxylic acid (Qian, 2016), and pyruvate and lactate (Johnson and Beckham, 2015). Also, lipid production was achieved in *Rhodococci* (Kosa and Ragauskas, 2012).

To develop a microbial chassis for coupling the utilization of biomass-derived aromatics with product synthesis, *Pseudomonas* spp. is an attractive candidate due to its versatile metabolism of aromatics (Weimer et al., 2020). These ubiquitously found Gram-negative bacteria have a broad substrate spectrum, including sugars, aromatics, hydrocarbons, and xenobiotics (Cao et al., 2009). The ability of high organic

* Corresponding author.

E-mail address: lars.blank@rwth-aachen.de (L.M. Blank).

<https://doi.org/10.1016/j.mec.2022.e00202>

Received 13 May 2022; Received in revised form 1 July 2022; Accepted 27 July 2022

Available online 10 August 2022

2214-0301/© 2022 The Authors. Published by Elsevier B.V. on behalf of International Metabolic Engineering Society. This is an open access article under the CC BY-NC-ND license (<http://creativecommons.org/licenses/by-nc-nd/4.0/>).

solvent tolerance makes some strains suitable hosts for specific catalytic tasks in industrial applications (Heipieper and Bont, 1994). Pseudomonads have been employed in academia and increasingly in the industry to produce a plenitude of valuable chemicals, including aromatics, polyketides, terpenoids, and glycolipids. Among these products, biosurfactants such as rhamnolipids are industrialized using *P. putida* as a host due to their immense range of applications in areas such as bioremediation, oil recovery, food processing, cosmetics, medicine, and agriculture (Borah et al., 2016; Husain, 2008; Magalhães and Nitschke, 2013; Rodrigues et al., 2006; Roy et al., 2015).

High-yield rhamnolipid production is currently reported in plenty of studies with the natural producer *Pseudomonas aeruginosa* (Müller et al., 2011), but the major drawback of this strain is that it is an opportunistic human pathogen. Therefore, there is a need for heterologous gene expression in non-pathogenic strains. Various studies involved expressing *rhlAB* genes from *P. aeruginosa* in non-pathogenic strains to produce rhamnolipids. For instance, in *Burkholderia kururiensis*, 5.6 g l⁻¹ rhamnolipids were produced from glycerol (Tavares et al., 2013). With glucose as substrate, *E. coli* produced 55–65 mg l⁻¹ of rhamnolipids (Haba et al., 2000). Additionally, including the *rmlBDAC* operon to increase rhamnose availability led to 120 mg l⁻¹ of rhamnolipids (Cabrera-Valladares et al., 2006). Germer et al. (2020) reported the production of 200 mg l⁻¹ HAAs, the lipid precursor for rhamnolipids. In the first recombinant study on rhamnolipid production using *P. fluorescens* and *P. putida*, 0.25 g l⁻¹ and 0.6 g l⁻¹ of products were reported, respectively (Ochsner et al., 1995). Rhamnolipid composition was altered using the *rhlAB* operon from *Burkholderia glumae* in *P. putida* KT2440, resulting in long-chain rhamnolipids (Wittgens et al., 2018).

Other than conventional substrates such as glucose, glycerol, and plant oils, many reports use renewable resources and industrial waste to produce rhamnolipids. Mostly different strains of *P. aeruginosa* have been used so far. Rhamnolipid titres of 200 mg l⁻¹ was achieved from olive oil mill waste (Moya Ramírez et al., 2015). Also using waste canola oil as substrate, 3 g l⁻¹ of rhamnolipids was reported (Pérez-Armendáriz et al., 2019). Furthermore, when grown on diesel and kerosene, 1 g l⁻¹ and 700 mg l⁻¹ of rhamnolipids were produced, respectively, using *P. aeruginosa* J4 (Wei et al., 2005). When cultivated on waste cooking oil, *P. aeruginosa* M4 produced 120 mg l⁻¹ of rhamnolipids (Shi et al., 2021). Recently, rhamnolipid production using plastic monomers as a carbon source was reported (Tiso et al., 2021; Utomo et al., 2020). To the best of our knowledge, there are no reports on rhamnolipid biosynthesis from biomass-derived aromatics as a novel carbon source.

In order to develop a microbial chassis for the production of rhamnolipids, *Pseudomonas taiwanensis* VLB120 is a promising candidate. Generally, hydrolysate of lignocellulosic biomass would contain pentoses from hemicellulose. For xylose being the most predominant building block of hemicellulose, there have been reports for engineering *P. putida* KT2440 for its utilization by heterologous expression of *xylAB* genes from *E. Coli* (Wang, et al., 2019). But the major advantage of using VLB120 is that it can natively use xylose as a substrate without the need for engineering (Köhler et al., 2015). Also, VLB120 has an important trait of high solvent tolerance that is desirable for industrial applications (Gross et al., 2010; Volmer et al., 2014). Additionally, this organism has the ability to do bioconversion using renewable substrates like glycerol (Lenzen et al., 2019). These attributes make them a suitable host for metabolic engineering. Various studies report the use of this strain as a production host for the biosynthesis of value-added products such as 4-hydroxybenzoate (Lenzen et al., 2019), n-octanol (Gross et al., 2013), phenol (Wynands, 2018), and isobutyric acid and isobutanol (Lang et al., 2014).

In this study, a metabolically engineered *P. taiwanensis* VLB120 was developed to grow efficiently on chosen biomass-derived aromatics 4-coumarate, ferulate, 4-hydroxy benzoate and vanillate. Out of all these aromatics, the wild type strain was able to grow natively on 4-hydroxy benzoate and vanillate. For growth on 4-coumarate and ferulate, the pathway genes necessary for the degradation of these aromatics were

integrated into the genome. Further, to enhance growth on non-native substrates, adaptive laboratory evolution was performed to achieve better tolerance. Whole genome sequencing was done to understand the mechanism at the genetic level that resulted in the enhanced phenotype. Finally, the evolved strain with increased tolerance was equipped with the required pathway genes for the production of rhamnolipids. Overall, this study demonstrated the utilization of biomass-derived aromatics for the production of value-added chemicals.

2. Materials and methods

2.1. Chemicals

Unless otherwise stated, all chemicals used in this work were purchased from Sigma Aldrich (Taufkirchen, Germany) or Carl Roth (Karlsruhe, Germany).

2.2. Strains and culture conditions

All the bacterial strains used in this study are listed in Table 1. To cultivate *E. coli* strains, LB medium containing 10 g l⁻¹ peptone, 5 g l⁻¹ sodium chloride, and 5 g l⁻¹ yeast extract was used. Plates were prepared by adding 1.5% agar (w/v) to the medium before autoclaving. For

Table 1
List of strains used in this study.

Strains	Characteristics	References
<i>E. coli</i> PIR1	F ⁻ Δ lac169 rpoS(Am) robA1 creC510 hsdR514 endA recA1uidA(Δ MluI)::pir-116; host for oriV(R6K) vectors in high copy number	Thermo Fisher Scientific
<i>E. coli</i> HB101 pRK2013	SmR, hsdR-M+, proA2, leuB6, thi-1, recA; harboring plasmid pRK2013	Ditta et al., (1980)
<i>E. coli</i> DH5 α pSW-2	DH5 α harboring plasmid pSW-2 encoding I-SceI nuclease tool for genomic deletion	Martínez-García and de Lorenzo, (2011)
<i>E. coli</i> pBELK ferulic s	Mini-Tn5 delivery vector harboring genes <i>ech</i> , <i>vdh</i> , and <i>fcs</i> from <i>P. putida</i> S12	Lenzen et al., (2019)
<i>E. coli</i> PIR2 pEMG-actP	PIR2 harboring plasmid pEMG-actP	this study
<i>E. coli</i> PIR2 pEMG-paaA	PIR2 harboring plasmid pEMG-paaA	this study
<i>E. coli</i> PIR2 pBG14ffg	PIR2 harboring Tn7 delivery vector pBG14ffg; containing BCD2-msfgfp fusion	Köbbing, (2020)
<i>E. coli</i> DH5 α λ pir pSK02	DH5 α λ pir harboring Tn7 delivery vector pSK02 for chromosomal integration; containing <i>rhlAB</i> genes from <i>P. aeruginosa</i> PA01	Bator et al., (2020)
<i>P. taiwanensis</i> VLB120	Wild type	(Panke, S., G. 1998)
<i>P. taiwanensis</i> VLB120 VS1	<i>P. taiwanensis</i> VLB120 carrying genes <i>ech</i> , <i>vdh</i> , and <i>fcs</i> genomically integrated via Tn5 transposon.	this study
<i>P. taiwanensis</i> VLB120 VS2	<i>P. taiwanensis</i> VLB120VS1 strain evolved in coumarate and ferulate mixture	this study
<i>P. taiwanensis</i> VLB120 VS3	<i>P. taiwanensis</i> VLB120 VS1 strain harboring Tn7 delivery vector pSK02 for chromosomal integration; containing <i>rhlAB</i> genes from <i>P. aeruginosa</i> PA01	this study
<i>P. taiwanensis</i> VLB120 VS1 Δ actP	<i>P. taiwanensis</i> VLB120 VS1 with <i>actP</i> gene knocked out	this study
<i>P. taiwanensis</i> VLB120 VS1 Δ paaA	<i>P. taiwanensis</i> VLB120 VS1 with <i>paaA</i> gene knocked out	this study
<i>P. taiwanensis</i> VLB120 VS1 paaA overexpression	<i>P. taiwanensis</i> VLB120 VS1 containing genomically integrated paaA gene	this study

selection on plates, respective antibiotics were supplemented into the medium. The antibiotic concentration of 50 mg l⁻¹ kanamycin and 10 mg l⁻¹ tetracycline was used. The cells were incubated at 37 °C and 300 rpm for cultivation in shake flasks. All *Pseudomonas* strains were grown on LB or cetrinide agar plates with the respective antibiotic for selection at 30 °C. The working volume of the shake flask was always maintained at 10% of the flask volume for all the strains throughout the studies.

For all growth and production experiments with *Pseudomonas* strains, a mineral salt medium (MSM) (Hartsmans et al., 1989) was used. MSM contains buffer: 11.64 g l⁻¹ K₂HPO₄ and 4.89 g l⁻¹ NaH₂PO₄, nitrogen source: 2 g l⁻¹ (NH₄)₂SO₄ and trace elements: 100 mg l⁻¹ MgCl₂ • 6 H₂O, 10 mg l⁻¹ EDTA, 2 mg l⁻¹ ZnSO₄ • 7 H₂O, 1 mg l⁻¹ CaCl₂ • 2 H₂O, 0.2 mg l⁻¹ Na₂MoO₄ • 2 H₂O, 0.2 mg l⁻¹ CuSO₄ • 5 H₂O, 5 mg l⁻¹ FeSO₄ • 7 H₂O, 0.4 mg l⁻¹ CoCl₂ • 6 H₂O, and 1 mg l⁻¹ MnCl₂ • 2 H₂O. Two precultures were prepared for all the cultivation experiments with 24-well System Duetz plates (Duetz et al., 2000) and shake flasks. The first preculture was prepared by cultivating the cells in LB medium from a glycerol stock or a freshly prepared LB plate and grown overnight at 30 °C and 300 rpm. The second preculture was prepared with MSM containing 20 mM glucose as a carbon source. 10 mM ferulate was used with MSM in the second preculture to reduce longer lag phases in aromatic substrates. The precultures were incubated at 30 °C and 300 rpm for 15–20 h. The cells were harvested by centrifuging at 5,000 rpm at 4 °C for 15 min and washed with 0.9% NaCl. The main culture was inoculated with a final OD₆₀₀ of 0.05–0.1 from the preculture. In System Duetz plates, fresh medium was supplemented with 0.2 mM IPTG to induce the expression of the genes encoding the ferulate degradation pathway and incubated at 30 °C and 300 rpm. This procedure was followed for shake flask cultivations as well.

2.3. Adaptive laboratory evolution

The *Pseudomonas taiwanensis* VLB120 VS1 strain was grown in MSM with biomass-derived aromatics as the sole carbon source at 30 °C and 300 rpm for adaptive laboratory evolution. Under identical conditions, each experimental condition was carried out simultaneously in 100 mL Erlenmeyer flasks with 10% working volume. The ALE experiment was performed in biological triplicates in parallel for each condition. The strain was adapted with coumarate and ferulate mixture. OD₆₀₀ was measured daily until it reached an OD above 1, after which it was reinoculated into a fresh medium starting at OD₆₀₀ of 0.1. This procedure was repeated sequentially for 42 days (up to 250 generations) by a step-wise increase in the concentration of aromatics. Samples were stored at –80 °C before every serial passage.

2.4. Recombinant DNA techniques

All plasmids were designed using NEBuilder Assembly Tool (New England Biolabs, USA) or Clone Manager Professional (Sci-Ed, Denver, USA) and procured from Eurofins Genomics (Ebersberg, Germany). Plasmids were constructed using Gibson assembly by NEBuilder HiFi DNA Assembly. Plasmid DNA isolation was done using the Monarch Plasmid Miniprep Kit (New England Biolabs, Ipswich, MA, USA) from overnight *E. coli* cultures. Plasmids were transferred into *E. coli* using heat shock and transformation in *Pseudomonas* was performed using conjugation through triparental mating as described by Wynands et al. (2018) or electroporation. Electroporation was done using a GenePulser Xcell (BioRad, Hercules, CA, USA) (settings: 2 mm cuvette gap, 2.5 kV, 200 Ω, 25 μF). Cetrinide agar plates with respective antibiotics were used for the selection of *Pseudomonas*. The method described by Martiñez-García and de Lorenzo (2011) was used for knocking out genes. Vector pEMG containing TS1 and TS2 flanking regions of the gene to be deleted was conjugated into the recipient strain, and correct integration was confirmed using colony PCR. Plasmid pSW-2 encoding enzyme I-SceI was used, and gene deletion was confirmed by colony PCR followed by DNA sequencing. Using a Tn7-based calibrated promoter

system, integration of genes was done using methods described in Zobel et al. (2015). All the cloning steps were verified by colony PCR using OneTaq DNA polymerase (New England Biolabs, Ipswich, USA). Genes *ech*, *vdh* and *fcs* for upstream catabolism of ferulate and 4-coumarate were genomically integrated into the wild type strain *P. taiwanensis* VLB120 via Tn5 mini-transposon system developed by Nikel and de Lorenzo (2013) using plasmid pBELK_ferulic_s (Lenzen et al., 2019). Expression of those genes took place under the control of the IPTG-inducible P_{trc} promoter. All the primers used in this study can be found in the Table S1.

2.5. Analytical methods

Biomass concentration was measured using spectrophotometer (GE Healthcare, Chicago, IL, USA) at 600 nm and converted to dry cellular weight by using a standard curve (1 OD₆₀₀ = 0.505 g l⁻¹ of dry cellular weight). Maximum specific growth rate (h⁻¹) was calculated from the plot of logarithm of biomass in the culture against cultivation time considering the exponential phase. For cultivation broth analysis, samples were collected by centrifugation at 5,000 rpm for 2 min, and the supernatant was stored at –20 °C. Bacterial growth was tracked using the Growth Profiler® (Enzygscreen, Heemstede, Netherlands).

Rhamnolipid analytics was performed using reversed-phase high-performance liquid chromatography (RP-HPLC) connected to a Charged Aerosol Detector (CAD) as developed by (Behrens et al., 2016a). Compounds were analyzed using a NUCLEODUR C18 Gravity, 3 μm, 4.6 × 150 mm column (Macherey-Nagel GmbH & Co. KG, Düren, Germany) maintained at an oven temperature of 40 °C and a flow rate of 1 ml min⁻¹. A Corona-charged aerosol detector (CAD) was used to detect rhamnolipids, connected to an HPLC system Ultimate 3000 (Thermo Fisher Scientific Inc., Waltham, MA, USA). Five microliters of the sample were injected. A binary gradient of 0.2% (v/v) formic acid in water and acetonitrile was used. Initially, the acetonitrile concentration was linearly increased from 70% to 100% between 1 min and 9 min, and then linearly decreased back to 70% between 11 min and 12 min. Each measurement was performed in 15 min. The chain length of rhamnolipid was determined using HPLC coupled with a tandem Mass Spectrometry LC-MS/MS as described in (Behrens et al., 2016b). The rhamnolipid concentration of *P. taiwanensis* cultures was measured after 3 days of cultivation. About 1 ml of the sample from culture was centrifuged for 5 min at 17,000g. 500 μl of the supernatant were subsequently mixed with 500 μL of acetonitrile and stored at 4 °C overnight for subsequent HPLC analysis.

2.6. Genome sequencing

Isolation of genomic DNA for whole-genome sequencing was done using a High Pure PCR Template Preparation Kit (ROCHE life science, Basel, Switzerland). Sequencing results were analyzed using Integrative Genomics Viewer (IGV) (Thorvaldsdóttir et al., 2013).

3. Results and discussion

3.1. Establishing growth of *P. taiwanensis* VLB120 on biomass-derived aromatics

Pseudomonas have in-built machinery of enzymes and pathways to metabolize various biomass-derived aromatics (Paliwal et al., 2014). In order to develop a microbial chassis of *P. taiwanensis* VLB120 to utilize the aromatics, the presence of respective pathways for the catabolism of aromatics was revisited. *P. taiwanensis* VLB120 possesses *pobA* (PVLB_11545) that encodes a 4-hydroxybenzoate monooxygenase and *vanAB* (PVLB_10605, PVLB_10610) encoding a vanillate monooxygenase. Both these genes are responsible for converting 4-hydroxybenzoate and vanillate to protocatechuate. However, *P. taiwanensis* VLB120 does not possess the metabolic pathway genes coding for the

feruloyl-CoA synthetase (*fcs*), enoyl-CoA hydratase (*ech*), and vanillin dehydrogenase (*vdh*), required for the degradation of ferulate and 4-coumarate. Therefore, wild type *P. taiwanensis* VLB120 grew on 4-hydroxybenzoate and vanillate but not on 4-coumarate and ferulate (Supplementary Fig. 1). In order to utilize ferulate as well as 4-coumarate, heterologous genes *fcs*, *ech*, and *vdh* from the ferulic operon of *P. putida* S12 were genomically integrated into wild type *P. taiwanensis* VLB120 using the Tn5 mini-transposon system (Nikel and de Lorenzo, 2013; Lenzen et al., 2019). Both ferulate and 4-coumarate are degraded using the protocatechuate branch of β -ketoacid pathway with vanillate as intermediate for ferulate and 4-hydroxybenzoate for 4-coumarate, respectively (Ravi et al., 2017). After conjugation, three clones were randomly picked from selective plates. Since all the clones grew in LB medium with the same performance (data not shown), it was assumed that neither of the integration sites had a negative impact on overall cell fitness. By the same token, we also excluded a direct relation between the disrupted genes and the aromatic catabolic pathway. Therefore, one of the clones was taken for all further experiments, referred to as *P. taiwanensis* VLB120 VS1.

After introducing the genes for ferulate and 4-coumarate degradation, the growth of the strain *P. taiwanensis* VLB120 VS1 was investigated in MSM containing 10 mM glucose equivalent to individual substrates, as shown in Fig. 1. Since ferulate and 4-coumarate are the upstream compound in the metabolic pathway, the preculture was grown with 10 mM ferulate and 4-coumarate as a sole carbon source, respectively. Growth rate was chosen as a key indicator for growth performance and substrate affinity. As the equivalent of 10 mM of glucose was applied for all aromatics, final G Values shown in Fig. 1 correspond to a final biomass of ~ 1.0 OD. Unlike the wild type strain, *P. taiwanensis* VLB120 VS1 was found to utilize and grow on all the aromatics. The growth on 4-hydroxybenzoate was highest with a growth rate of 0.36 h^{-1} , which was faster than on glucose (0.3 h^{-1}), while cells grew slower on vanillate (0.17 h^{-1}). Growth rates in the presence of 4-coumarate (0.07 h^{-1}) and ferulate (0.05 h^{-1}) were low, with extended lag phases (7 h for 4-coumarate and 9 h for ferulate). Nonetheless, integration of the peripheral genes *fcs*, *ech*, and *vdh* rendered strain VLB120 VS1 capable of using major aromatics as the sole carbon source and generated a platform for their valorization.

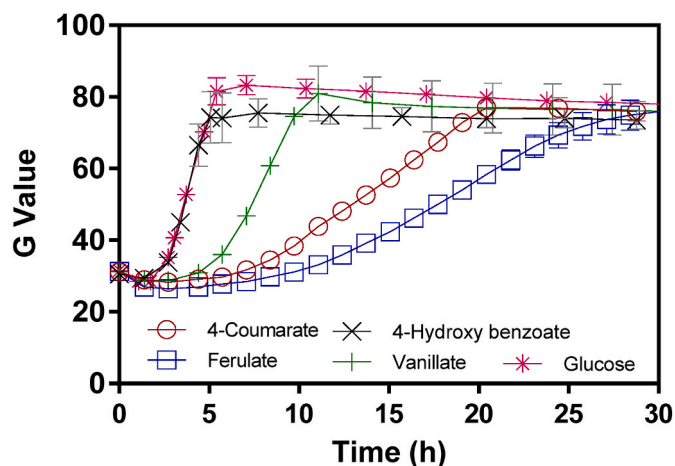


Fig. 1. Growth profiles of engineered Pseudomonas: *P. taiwanensis* VLB120 VS1 were cultivated in 24-well System Duetz plates in a Growth Profiler in MSM containing 10 mM glucose equivalent of each aromatic as the sole carbon source. The working volume of each well was 1.5 ml. Cells were maintained at 30 °C and 300 rpm. The values shown here are from biological triplicates, and error bars indicate the standard error of the mean.

3.2. *P. taiwanensis* VLB120 VS1 shows enhanced growth on ferulate and 4-coumarate after adaptive evolution

Generally, different biomass-derived aromatics exhibit different levels of toxicity towards the microorganisms. For instance, in *S. cerevisiae*, ferulate was found to have a toxicity limit of 1.8 mM, but 4-coumarate had a higher toxicity limit of 9.7 mM (Adeboye et al., 2014). Improvement of microbial traits can be accomplished by adaptive laboratory evolution (Sandberg et al., 2020). Using this non-rational and straightforward method, host properties linked to growth can be enhanced rapidly without knowing the exact genetic or metabolic basis beforehand. In order to improve the ability of *P. taiwanensis* VLB120 VS1 to assimilate ferulate and 4-coumarate, the strain was cultivated in the presence of these aromatics as mixed carbon sources. The experiment was carried out in three parallel shake flask cultivations. ALE was performed with MSM containing 4-coumarate and ferulate mixture for about 220 generations for 42 days (Fig. S2). After screening 50 mutants from the evolution approach, a strain with the highest growth rate on ferulate and 4-coumarate was selected and referred to as *P. taiwanensis* VLB120 VS2 (data not shown).

The growth of the evolved VLB120 VS2 strain was investigated at varying concentrations compared to the non-evolved strain VLB120 VS1. The evaluation was done with individual substrates at different concentrations ranging from 5 mM to 30 mM. While cultivating cells in MSM, the lag phase in 4-coumarate was shortened by 89% and by 80% in ferulate (Fig. S3- A, B, C, D). An 80% reduction in lag phase was also observed when VLB120 VS2 was grown on a mixture of substrates (Fig. S3- E, F). The growth rates improved up to 78% in 4-coumarate, 82% in ferulate, and 67% in the mixture (Fig. S4). Growth of the evolved VLB120 VS2 strain was also investigated under 4-hydroxybenzoate and vanillate conditions. However, no considerable improvement in the lag phase or growth rate could be observed in these aromatics.

3.3. Analysis by whole genome sequencing

To investigate the molecular basis of the improved growth of *P. taiwanensis* VLB120 VS2 on ferulate and 4-coumarate as sole carbon sources, the genome of this strain and the operon consisting of degradative ferulic genes *fcs*, *ech*, and *vdh*, were isolated and sequenced. No mutations were found in the ferulic promoter region and the respective genes. Instead, strong accumulation of mutations was found within two loci of the host genome, including single nucleotide exchanges and insertions (Table 2). One locus was found to be coding for the ActP transporter (PVLB_12535). This sodium:solute symporter is involved in the specific transport of acetate and other small aliphatic monocarboxylates (Gimenez et al., 2003). Its expression is controlled by the CrbS/R regulon, and wherein *actP* is co-expressed with *acs*. The *acs* gene codes for acetyl-CoA synthase that uses acetate as a substrate (Jacob et al., 2017; Sepulveda and Lupas, 2017). We identified nine single-nucleotide exchanges resulting in amino acid substitutions and a frameshift caused by the insertion of seven base pairs within the open reading frame of *actP*. The second mutational hotspot was found to be *paaA*. This gene is a part of the *paaABCDE* operon that codes for phenylacetyl-CoA oxygenase of the phenylalanine and phenylacetate catabolic pathway that uses phenylacetyl-CoA as a substrate (Erb et al.,

Table 2

Key mutations found in whole-genome sequencing of *P. taiwanensis* VLB120 VS2.

Position in the genome	Type of mutation	No. of mutations	Gene/gene product
2769737 - 2771299	SNP, INDEL	10	actP/acetate permease (cation/acetate symporter)
2774408 - 2775397	SNP	5	paaA/phenylacetate - CoA oxygenase subunit

2008; Fernández et al., 2006; Teufel et al., 2010). There were five nucleotide exchanges identified in this gene. In addition to these two genes, there were further mutations, including SNPs and INDELS in the intergenic regions and the region coding for hypothetical proteins in the genome (Table S2). In a similar study, an evolution experiment was performed in 4-coumarate and ferulate using *P. putida* KT2440. This study revealed frequent mutations in a gene coding for a hypothetical protein PP_3350 and a gene *tigB* that codes for an efflux pump membrane transporter along with mutations in genes involved in flagellar movement and transcriptional regulation (Mohamed et al., 2020). The gene targets with similar identity of that in KT2440 can also be targeted for reverse engineering in order to achieve efficient utilization of biomass-derived aromatics.

3.4. Reverse engineering of VLB120 VS1

Using the above information from the genome sequencing, we targeted the genes *actP* and *paaA* for reverse engineering of the *P. taiwanensis* VLB120 VS1 strain. The mutations in *actP* show that the gene had lost its function in the evolved strain *P. taiwanensis* VLB120 VS2. Therefore, we knocked out the *actP* gene in the unevolved strain *P. taiwanensis* VLB120 VS1. Cultivation of VLB120 VS1 $\Delta actP$ in MSM containing 4-coumarate (Fig. 2A) or ferulate (Fig. 2B) showed an intermediate phenotype between the non-mutated strain VLB120 VS1 and evolved strain VLB120 VS2. However, the reason for the improved growth of VLB120 VS1 $\Delta actP$ on 4-coumarate and ferulate is not that obvious. As already mentioned, there is evidence of a coupled expression of the *ActP* transporter and the acetyl-CoA synthase *Acs* (Jacob et al., 2017; Sepulveda and Lupas, 2017). The absence of the transporter in strain VLB120 $\Delta actP$ may result in an increased CoA-SH pool due to decreased acetate intake and activity of *Acs*, which in turn can be exploited by feruloyl-CoA synthase for faster processing of 4-coumarate and ferulate in the peripheral pathway.

Upon targeting *paaA* for reverse engineering, it was not evident whether mutagenesis of *paaA* in the evolved strain caused a loss or gain of gene function since there was no frameshift mutation in the gene. Therefore, for evaluating loss of function, we knocked out *paaA*, thereby

generating mutant strain VLB120 VS1 $\Delta paaA$. For evaluating the gain of function, we genomically integrated a copy of the evolved *paaA* into the *attTn7* site of VLB120 VS1 for overexpression from a medium-strength constitutive promoter. The generated strain, VLB120 VS1 BG14d *paaA*, and its deficient counterpart, VLB120 $\Delta paaA$, were grown in MSM with 4-coumarate (Fig. 2C) or ferulate (Fig. 2D). In comparison to the non-mutated strain VLB120 VS1, the overexpression strain VLB120 VS1 BG14d *paaA* exhibited biomass formation with an increased growth rate as well as a shorter lag phase, but not to the extent of the evolved strain VLB120 VS2. Conversely, knockout of *paaA* in strain VLB120 VS1 had a negative effect on the growth on aromatics, in that mutant strain VLB120 VS1 $\Delta paaA$ grew even slower with a more prolonged lag phase than the non-evolved strain. We concluded from these observations that *paaA* is involved in the catabolic breakdown of 4-coumarate and ferulate. It encodes the PaaA subunit of an enoyl-CoA hydratase complex using phenylacetyl-CoA as a substrate. Due to its structural similarities to the activated forms of ferulate and 4-coumarate, feruloyl-CoA and 4-coumaroyl-CoA, and the extremely slow growth of the *paaA* deficient strain, it can be assumed that PaaA acts in parallel to Ech as being part of the peripheral catabolic pathway. Overexpression of *paaA*, in turn, leads to higher enzyme activity and thus to faster processing, whereas it remains to be demonstrated that mutation in the evolved *paaA* version, in particular, has the highest effect. Also the role of *paaA* in the catabolism of 4-coumarate and ferulate can be understood by knocking out *ech* gene in the evolved strain and check if *paaA* can replace its function.

In summary, Fig. 3 shows the growth on all the strains. Both *actP* knockout and *paaA* overexpression results in enhanced catabolic processing of ferulate and 4-coumarate. Both reverse engineering modifications show an intermediate phenotype between non-evolved (VLB120 VS1) and evolved strain (VLB120 VS2); a synergistic effect of these two key components can be anticipated. Therefore further metabolic engineering was therefore attempted with the VLB120 VS2 strain, which had the best phenotypic characteristics compared to the wild type (VLB120 VS1) and the reverse-engineered strains.

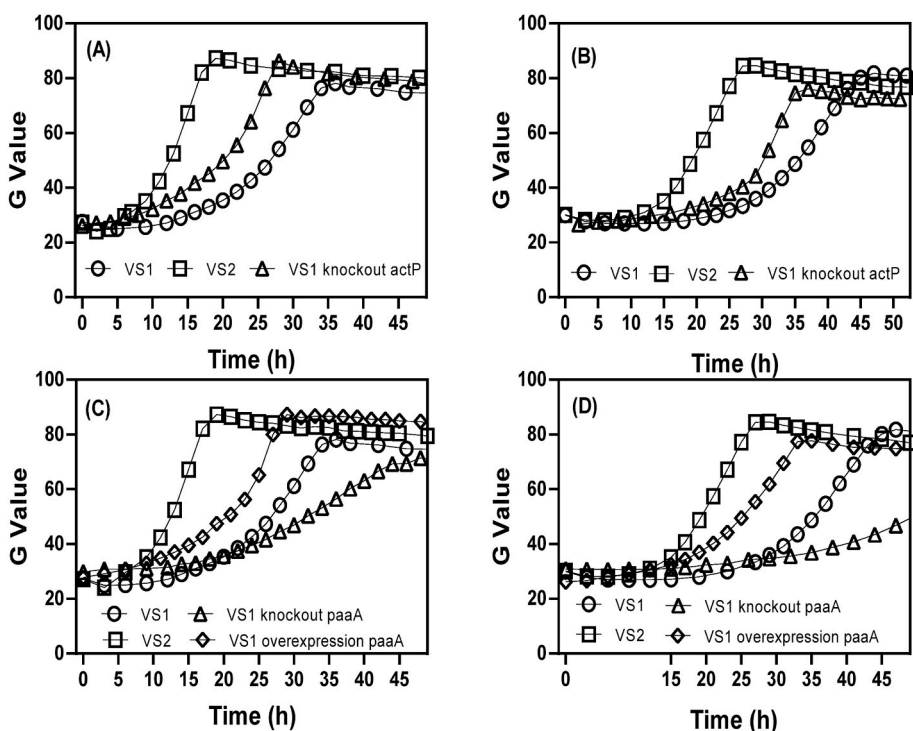


Fig. 2. Cultivation experiments were carried out in the growth profiler. Growth profiles were monitored for the strains VLB120 VS1, VLB120 VS2, and VLB120 VS1 $\Delta actP$ in 4-coumarate (A) and ferulate (B) as the sole carbon sources. Also, the growth of strains VLB120 VS1 $\Delta paaA$ and VLB120 VS1 *paaA* overexpression in 4-coumarate (C) and ferulate (D) was monitored. All the experiments were performed with biological duplicates, and error bars represent the standard error of the mean.

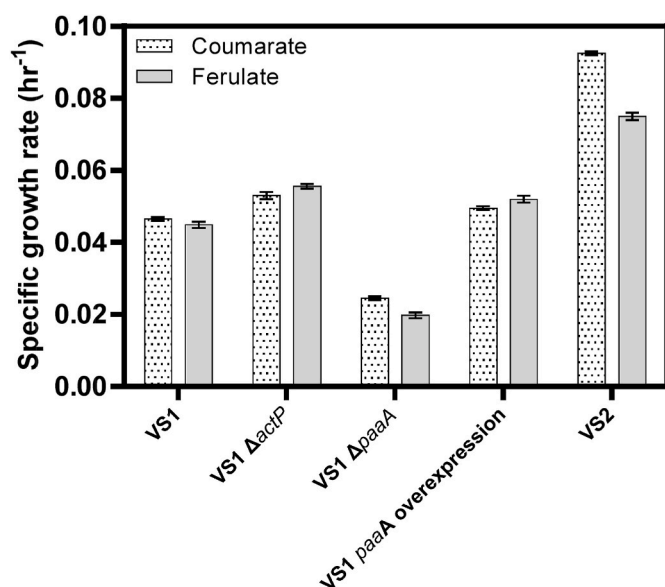


Fig. 3. Comparison of specific growth rates of the reverse-engineered strains along with non-evolved and evolved strains. All the experiments were performed with biological duplicates, and error bars represent the standard error of the mean.

3.5. Rhamnolipid production

Rhamnolipids are a promising alternative to chemically derived surfactants due to their biodegradability, low toxicity, and their ability for metal ion complexation. Several organisms have been utilized as hosts for microbial rhamnolipid production, among which *Pseudomonas* species are predominant (Tiso et al., 2017). Mainly sugars or plant oils were used as the substrate, with plastic monomers as an exception (Utomo et al., 2020). This study uses biomass-derived aromatics as substrates since *P. taiwanensis* VLB120 was successfully used as a production host for aromatics from sugars (Lenzen et al., 2019; Wynands, 2018; Wynands et al., 2019). The primary objective of this study was to explore the utilization of aromatics as carbon sources for rhamnolipid production. We, therefore, established *de novo* mono-rhamnolipid production in our evolved strain *P. taiwanensis* VLB120 VS2. Here, the two genes *rhlA* and *rhlB* from *P. aeruginosa* were introduced. *rhlA* encodes an acyltransferase responsible for generating 3-(hydroxyalkanoxy)alkanoic acid (HAA) derived from the fatty acid *de novo* synthesis. This activated β -hydroxy fatty acid is then linked to rhamnose via dTDP-rhamnose with the help of a rhamnosyltransferase encoded by *rhlB*. For aromatic-based rhamnolipid production, the evolved strain *P. taiwanensis* VLB120 VS2 was equipped with plasmid pSK02 harboring *rhlAB* genes from *P. aeruginosa* under expression control of a constitutive stacked promoter (Bator et al., 2020). The best producing strain was visually identified after conjugation by formation of the largest halos-producing strain on the cetrimide blood agar plates due to hemolytic activity (Fig. S5). The newly-engineered strain for rhamnolipid production was labelled as VLB120 VS3. The overall pathway for the production of rhamnolipid biosynthesis from biomass-derived aromatics

is represented in Fig. S6.

All the aromatics tested and their corresponding rhamnolipids production is listed in Table 3. Among the tested aromatic substrates, growth on ferulate and 4-coumarate generated the highest rhamnolipid titer ($\sim 0.43 \text{ g l}^{-1}$). Approximately half of this amount was obtained with vanillate as substrate, whereas 4-hydroxybenzoate yielded the least. Wittgens et al. (2012) reported a growth-independent rhamnolipid production of an engineered *P. putida* strain during growth on LB medium supplemented with glucose, wherein components of the LB medium are assimilated for biomass formation, and glucose was used by the cell for rhamnolipid biosynthesis. In contrast to this system, the aromatics used here act as a carbon source for cell growth and are channelled into product formation. Catabolic breakdown of ferulate as well as 4-coumarate is initiated by their activation to acyl-CoAs catalyzed by feruloyl-CoA synthetase encoded by the *fcs* gene. Subsequent enzymatic breakdown by enoyl-CoA hydratase, the gene product of *ech*, then releases one molecule acetyl-CoA per molecule ferulate and 4-coumarate, respectively. The additional gain of acetyl-CoA during this reaction may be beneficial for rhamnolipid precursor production within *de novo* fatty acid biosynthesis and therefore explain higher rhamnolipid titers reached during growth on ferulate and 4-coumarate. While dealing with a mixture of all these aromatics, a maximum titer of about 0.21 g l^{-1} was achieved. This was comparable to that of rhamnolipid production with individual aromatics such as coumarate or ferulate. This might be due to the effect of catabolite repression that was observed when dealing with multiple substrates (Fig. S7). Since there is the sequential utilization of hydroxybenzoate and vanillate in the initial phase, followed by coumarate and ferulate, it is most likely that the culture growing on a mixture of these substrates utilizes hydroxybenzoate and vanillate more for biomass production while coumarate and ferulate are utilized more for rhamnolipid production. One can perhaps achieve simultaneous utilization of all the substrates and better productivity by eliminating the *crc* gene, a global regulator of carbon catabolite repression (Johnson et al., 2017).

The highest Cmol yield was achieved during growth on 4-coumarate, corresponding to $0.22 \text{ C}_{\text{mol}}/\text{C}_{\text{mol}}$. One production strain engineered by (Wittgens et al., 2012) produced 0.22 g l^{-1} mono-rhamnolipids in LB medium supplemented with 10 g l^{-1} glucose. Further improvement of production performance was achieved by using a PHA-negative mutant of *P. putida* deficient for the *phaC1* poly(3-hydroxyalkanoic acid) synthase 1. During *de novo* fatty acid biosynthesis, this enzyme catalyzes the formation of PHA from the precursor β -hydroxyaryl-CoA under specific environmental circumstances, e.g., nitrogen limitation. Competition of PHA accumulation and storage with rhamnolipid biosynthesis was prevented by knocking out the PHA synthase gene, leading to an almost seven-fold increase in mono-rhamnolipid titer. PHA synthesis is widespread among bacteria, and the *phaC1* gene can be found in the genome of *P. taiwanensis* VLB120 (PVLB_02155). Hence rendering strain VLB120 VS3 deficient for PHA accumulation will likely boost mono-rhamnolipid production from aromatics. However, with the setup established here, mono-rhamnolipid production in MSM from biomass-derived aromatics was shown to be feasible and even competitive with the use of glucose.

Table 3

Rhamnolipid production of *P. taiwanensis* VLB120 VS3. Production of rhamnolipid was carried out in MSM containing 10 mM of the respective biomass-derived aromatics as the sole carbon source in shake flask cultivations.

LDM	Biomass [g l^{-1}]	Rhamnolipid titer [g l^{-1}]	Yield ($\text{C}_{\text{mol}}/\text{C}_{\text{mol}}/\text{C}_{\text{substrate}}$)
Ferulate	1.76 ± 0.2	0.432 ± 0.022	0.22
4-Coumarate	2.1 ± 0.3	0.436 ± 0.006	0.27
Vanillate	1.8 ± 0.15	0.236 ± 0.004	0.14
4-Hydroxybenzoate	1.7 ± 0.16	0.131 ± 0.005	0.09
Mixture	1.8 ± 0.14	0.210 ± 0.015	0.06

4. Conclusion and outlook

This study has reported the successful use of biomass-derived aromatics for producing rhamnolipids using *P. taiwanensis* VLB120. This was done by using metabolic engineering approaches for aromatic substrate utilization. In this work, we have accomplished the utilization of ferulate and 4-coumarate by heterologous gene expression of ferulic operon genes *ech*, *fcs*, and *vdh*. This paved the way for using these compounds as substrates, which cannot be consumed by the wild type *P. taiwanensis* VLB120. Also, the growth on aromatics was improved using adaptive evolution. This was a promising non-rational strain engineering approach that resulted in enormous tolerance towards 4-coumarate and ferulate. With whole-genome sequencing, the genomic alterations during the ALE experiment could be investigated. The evolved strain *P. taiwanensis* VLB VS2 was successfully engineered to produce mono-rhamnolipids that predominantly consisted of the C10–C10 moiety. 4-coumarate and ferulate were preferred substrates with a titre of about 0.43 g l⁻¹. The titres we achieved were comparable to that of other unconventional substrates used for rhamnolipid production. Also, this proof of concept study can be applied for industrial applications that involve usage of lignocellulosic biomass. By employing an appropriate method of lignin depolymerization one can yield desired types of selective aromatics. For example, in the mild base-catalyzed depolymerization of corn stover at a temperature of about 120 °C and 2% NaOH, 4-coumarate was the most predominant aromatic compound of about 6 g l⁻¹ followed by ferulate of about 180 mg l⁻¹. Other compounds such as 4-hydroxybenzoate and vanillate were also present at minimal levels (Rodríguez et al., 2017). So, this study can be extended to valorize low molecular weight lignin compounds by bioconversion of these compounds to value-added products. Thus the use of aromatics as substrates for the production of valuable chemicals contributes to the vision of an integrated biorefinery that uses not only the sugars derived from biomass but also utilizes the untapped lignin.

Author contributions

V.S and C.L: Design of experiments. V.S and C.M: Perform experiments and analyze the results. A.B: Initiating collaboration and funding. V.S and C.L: Write and review the original draft. G.J and L.M.B: Review and edit the original draft, along with supervision and funding acquisition.

Declaration of competing interest

The authors declare that they have no known competing financial interests or personal relationships that could have appeared to influence the work reported in this paper.

Acknowledgments

This project (LIGFUEL) is funded as a part of the Inno Indigo Program funded by the German Federal Ministry of Education and Research and DBT, Ministry of Science and Technology, Government of India (Grant nos. 01DQ17015 and BT/IN/INNO-Indigo/32/GJ/2016–17). The laboratory of Lars M. Blank was also partially funded by the Deutsche Forschungsgemeinschaft (DFG, German Research Foundation) under Germany's Excellence Strategy within the Clusters of Excellence TMFB 236 and FSC 2186 'The Fuel Science Center'. We thank the Ministry of Human Resource Development, GOI, and UGC DAAD Indo-German Strategic Partnership for funding the fellowship to VS.

Appendix A. Supplementary data

Supplementary data to this article can be found online at <https://doi.org/10.1016/j.mec.2022.e00202>.

References

- Adeboye, P.T., Bettiga, M., Olsson, L., 2014. The chemical nature of phenolic compounds determines their toxicity and induces distinct physiological responses in *Saccharomyces cerevisiae* in lignocellulose hydrolysates. *Amb. Express* 4, 1–10. <https://doi.org/10.1186/s13568-014-0046-7>.
- Barton, N., Horbal, L., Starck, S., Kohlstedt, M., Luzhetskyy, A., Wittmann, C., 2018. Enabling the valorization of guaiacol-based lignin: integrated chemical and biochemical production of cis,cis-muconic acid using metabolically engineered *Amycolatopsis* sp ATCC 39116. *Metab. Eng.* 45, 200–210. <https://doi.org/10.1016/j.ymben.2017.12.001>.
- Bator, I., Wittgens, A., Rosenau, F., Tiso, T., Blank, L.M., 2020. Comparison of three xylose pathways in *Pseudomonas putida* KT2440 for the synthesis of valuable products. *Front. Bioeng. Biotechnol.* 7, 1–18. <https://doi.org/10.3389/fbioe.2019.00480>.
- Becker, J., Wittmann, C., 2019. A field of dreams: lignin valorization into chemicals, materials, fuels, and health-care products. *Biotechnol. Adv.* 37, 107360. <https://doi.org/10.1016/j.biotechadv.2019.02.016>.
- Behrens, B., Baune, M., Jungkeit, J., Tiso, T., Blank, L.M., Hayen, H., 2016a. High performance liquid chromatography-charged aerosol detection applying an inverse gradient for quantification of rhamnolipid biosurfactants. *J. Chromatogr. A* 1455, 125–132. <https://doi.org/10.1016/j.chroma.2016.05.079>.
- Behrens, B., Engelen, J., Tiso, T., Blank, L.M., Hayen, H., 2016b. Characterization of rhamnolipids by liquid chromatography/mass spectrometry after solid-phase extraction. *Anal. Bioanal. Chem.* 408, 2505–2514. <https://doi.org/10.1007/s00216-016-9353-y>.
- Borah, S.N., Goswami, D., Sarma, H.K., Cameotra, S.S., Deka, S., 2016. Rhamnolipid biosurfactant against *Fusarium verticillioides* to control stalk and ear rot disease of maize. *Front. Microbiol.* 7, 1–10. <https://doi.org/10.3389/fmicb.2016.01505>.
- Borrero-de Acuña, J.M., Gutierrez-Urrutia, I., Hidalgo-Dumont, C., Aravena-Carrasco, C., Orellana-Saez, M., Palominos-Gonzalez, N., van Duuren, J.B.J.H., Wagner, V., Gläser, L., Becker, J., Kohlstedt, M., Zaccani, F.C., Wittmann, C., Poblete-Castro, I., 2021. Channelling carbon flux through the meta-cleavage route for improved poly(3-hydroxyalkanoate) production from benzoate and lignin-based aromatics in *Pseudomonas putida* H. *Microb. Biotechnol.* 14, 2385–2402. <https://doi.org/10.1111/1751-7915.13705>.
- Cabrera-Valladares, N., Richardson, A.P., Olvera, C., Treviño, L.G., Déziel, E., Lépine, F., Soberón-Chávez, G., 2006. Monorhamnolipids and 3-(3-hydroxyalkanoxyloxy) alkanolic acids (HAAs) production using *Escherichia coli* as a heterologous host. *Appl. Microbiol. Biotechnol.* 73, 187–194. <https://doi.org/10.1007/s00253-006-0468-5>.
- Cao, B., Nagarajan, K., Loh, K.C., 2009. Biodegradation of aromatic compounds: current status and opportunities for biomolecular approaches. *Appl. Microbiol. Biotechnol.* 85, 207–228. <https://doi.org/10.1007/s00253-009-2192-4>.
- Ditta, G., Stanfield, S., Corbin, D., Helinski, D.R., 1980. Broad host range DNA cloning system for Gram-negative bacteria: construction of a gene bank of *Rhizobium meliloti*. *Proc. Natl. Acad. Sci. U.S.A.* 77, 7347–7351. <https://doi.org/10.1073/pnas.77.12.7347>.
- Duetz, W.A., Rüedi, L., Hermann, R., O'Connor, K., Büchs, J., Witholt, B., 2000. Methods for intense aeration, growth, storage, and replication of bacterial strains in microtiter plates. *Appl. Environ. Microbiol.* 66, 2641–2646. <https://doi.org/10.1128/AEM.66.6.2641-2646.2000>.
- Elmore, J.R., Dexter, G.N., Salvachúa, D., Martínez-baird, J., Hatmaker, E.A., Huenemann, J.D., Klingeman, D.M., V, G.L.P., Peterson, D.J., Singer, C., Beckham G. T., Guss, A.M., n.d. Production of itaconic acid from alkali pretreated lignin by dynamic two stage bioconversion. *Nat. Commun.* <https://doi.org/10.1038/s41467-021-22556-8>.
- Erb, T.J., Ismail, W., Fuchs, G., 2008. Phenylacetate metabolism in thermophiles: characterization of phenylacetate-CoA ligase, the initial enzyme of the hybrid pathway in *Thermus thermophilus*. *Curr. Microbiol.* 57, 27–32. <https://doi.org/10.1007/s00284-008-9147-3>.
- Fernández, C., Ferrández, A., Miñambres, B., Díaz, E., García, J.L., 2006. Genetic characterization of the phenylacetyl-coenzyme A oxygenase from the aerobic phenylacetic acid degradation pathway of *Escherichia coli*. *Appl. Environ. Microbiol.* 72, 7422–7426. <https://doi.org/10.1128/AEM.01550-06>.
- Germer, A., Tiso, T., Müller, C., Behrens, B., Vosse, C., Scholz, K., Froning, M., Hayen, H., Blank, L.M., 2020. Exploiting the natural diversity of RhIA acyltransferases for the synthesis of the rhamnolipid precursor 3-(3-Hydroxyalkanoxyloxy)Alkanolic acid. *Appl. Environ. Microbiol.* 86, 1–16. <https://doi.org/10.1128/AEM.02317-19>.
- Gimenez, R., Nuñez, M.F., Badia, J., Aguilar, J., Baldoma, L., 2003. The gene *ycjG*, cotranscribed with the gene *acs*, encodes an acetate permease in *Escherichia coli*. *J. Bacteriol.* 185, 6448–6455. <https://doi.org/10.1128/JB.185.21.6448-6455.2003>.
- Gross, et al., 2010. Characterization of a biofilm membrane reactor and its prospects for fine chemical synthesis. *Biotechnology and Bioengineering* 105 (4). <https://doi.org/10.1002/bit.22584>.
- Gross, R., Buehler, K., Schmid, A., 2013. Engineered catalytic biofilms for continuous large scale production of n-octanol and (S)-styrene oxide. *Biotechnol. Bioeng.* 110, 424–436. <https://doi.org/10.1002/bit.24629>.
- Haba, E., Espuny, M.J., Busquets, M., Manresa, A., 2000. Screening and production of rhamnolipids by *Pseudomonas aeruginosa* 47T2 NCIB 40044 from waste frying oils. *J. Appl. Microbiol.* 88, 379–387. <https://doi.org/10.1046/j.1365-2672.2000.00961.x>.
- Hartmans, et al., 1989. Metabolism of styrene oxide and 2-phenylethanol in the styrene-degrading *Xanthobacter* Strain 124X. *Appl. Environ. Microbiol.* 55 (11).
- Heipieper, H.J., Bont, J. a M. De, 1994. Adaptation of *Pseudomonas putida* S12. *Appl. Environ. Microbiol.* 60, 4440–4444.

- Husain, S., 2008. Effect of surfactants on pyrene degradation by *Pseudomonas fluorescens* 29L. *World J. Microbiol. Biotechnol.* 24, 2411–2419. <https://doi.org/10.1007/s11274-008-9756-9>.
- Jacob, K., Rasmussen, A., Tyler, P., Servos, M.M., Sylla, M., Prado, C., Daniele, E., Sharp, J.S., Purdy, A.E., 2017. Regulation of acetyl-CoA synthetase transcription by the CrbS/R two-component system is conserved in genetically diverse environmental pathogens. *PLoS One* 12, 1–27. <https://doi.org/10.1371/journal.pone.0177825>.
- Johnson, C.W., Abraham, P.E., Linger, J.G., Khanna, P., Hettich, R.L., Beckham, G.T., 2017. Eliminating a global regulator of carbon catabolite repression enhances the conversion of aromatic lignin monomers to muconate in *Pseudomonas putida* KT2440. *Metab. Eng. Commun.* 5, 19–25. <https://doi.org/10.1016/j.meten.2017.05.002>.
- Johnson, C.W., Beckham, G.T., 2015. Aromatic catabolic pathway selection for optimal production of pyruvate and lactate from lignin. *Metab. Eng.* 28, 240–247. <https://doi.org/10.1016/j.ymben.2015.01.005>.
- Köbbing, S., 2020. Development of Synthetic Biology Tools for *Pseudomonas putida*.
- Köhler, K.A.K., Blank, L.M., Frick, O., Schmid, A., 2015. D-Xylose assimilation via the Weimberg pathway by solvent-tolerant *Pseudomonas taiwanensis* VLB120. *Environ. Microbiol.* 17, 156–170. <https://doi.org/10.1111/1462-2920.12537>.
- Kosa, M., Ragauskas, A.J., 2012. Bioconversion of lignin model compounds with oleaginous Rhodococci. *Appl. Microbiol. Biotechnol.* 93, 891–900. <https://doi.org/10.1007/s00253-011-3743-z>.
- Lang, K., Zierow, J., Buehler, K., Schmid, A., 2014. Metabolic engineering of *Pseudomonas* sp. strain VLB120 as platform biocatalyst for the production of isobutyric acid and other secondary metabolites. *Microb. Cell Factories* 13. <https://doi.org/10.1186/1475-2859-13-2>.
- Lenzen, C., Wynands, B., Otto, M., Bolzenius, J., Mennicken, P., Blank, L.M., Wierckx, N., 2019. High-yield production of 4-hydroxybenzoate from glucose or glycerol by an engineered *Pseudomonas taiwanensis* VLB120. *Front. Bioeng. Biotechnol.* 7, 1–17. <https://doi.org/10.3389/fbioe.2019.00130>.
- Magalhães, L., Nitschke, M., 2013. Antimicrobial activity of rhamnolipids against *Listeria monocytogenes* and their synergistic interaction with nisin. *Food Control* 29, 138–142. <https://doi.org/10.1016/j.foodcont.2012.06.009>.
- Martínez-García, E., de Lorenzo, V., 2011. Engineering multiple genomic deletions in Gram-negative bacteria: analysis of the multi-resistant antibiotic profile of *Pseudomonas putida* KT2440. *Environ. Microbiol.* 13, 2702–2716. <https://doi.org/10.1111/j.1462-2920.2011.02538.x>.
- Mohamed, E.T., Werner, A.Z., Salvachúa, D., Singer, C.A., Szostkiewicz, K., Rafael Jiménez-Díaz, M., Eng, T., Radi, M.S., Simmons, B.A., Mukhopadhyay, A., Herrgård, M.J., Singer, S.W., Beckham, G.T., Feist, A.M., 2020. Adaptive laboratory evolution of *Pseudomonas putida* KT2440 improves p-coumaric and ferulic acid catabolism and tolerance. *Metab. Eng. Commun.* 11. <https://doi.org/10.1016/j.mec.2020.e00143>.
- Moya Ramírez, I., Tsaousi, K., Rudden, M., Marchant, R., Jurado Alameda, E., García Román, M., Banat, I.M., 2015. Rhamnolipid and surfactin production from olive oil mill waste as sole carbon source. *Bioresour. Technol.* 198, 231–236. <https://doi.org/10.1016/j.biortech.2015.09.012>.
- Müller, M.M., Hörmann, B., Kugel, M., Syldatk, C., Hausmann, R., 2011. Evaluation of rhamnolipid production capacity of *Pseudomonas aeruginosa* PAO1 in comparison to the rhamnolipid over-producer strains DSM 7108 and DSM 2874. *Appl. Microbiol. Biotechnol.* 89, 585–592. <https://doi.org/10.1007/s00253-010-2901-z>.
- Nikel, P.I., de Lorenzo, V., 2013. Implantation of unmarked regulatory and metabolic modules in Gram-negative bacteria with specialised mini-transposon delivery vectors. *J. Biotechnol.* 163, 143–154. <https://doi.org/10.1016/j.jbiotec.2012.05.002>.
- Ochsner, U.A., Reiser, J., Fiechter, A., Witholt, B., 1995. Production of *Pseudomonas aeruginosa* rhamnolipid biosurfactants in heterologous hosts. *Appl. Environ. Microbiol.* 61, 3503–3506. <https://doi.org/10.1128/aem.61.9.3503-3506.1995>.
- Paliwal, et al., 2014. *Pseudomonasputida* CSV86: A Candidate Genome for Genetic Bioaugmentation. *PLOS one* 9 (1), e84000.
- Palmqvist, E., 2000. Fermentation of lignocellulosic hydrolysates. II: inhibitors and mechanisms of inhibition, 74, pp. 25–33.
- Panke, S., Witholt, B., Schmid, A., Wubbolts, M.G., 1998. Towards a biocatalyst for (S)-styrene oxide production: characterization of the styrene degradation pathway of *Pseudomonas* sp. strain VLB120. *Appl. Environ. Microbiol.* 64, 2032–2043, 1998. Towards a Biocatalyst for (64, 2032–2043).
- Pérez-Armendáriz, B., Cal-y-Mayor-Luna, C., El-Kassis, E.G., Ortega-Martínez, L.D., 2019. Use of waste canola oil as a low-cost substrate for rhamnolipid production using *Pseudomonas aeruginosa*. *AMB Express.* <https://doi.org/10.1186/s13568-019-0784-7>, 9.
- Qian, et al., 2016. Engineered microbial production of 2-pyrone-4,6-dicarboxylic acid from lignin residues for use as an. *Industrial Platform Chemical* 11, 6097–6109.
- Raj, A., Chandra, R., Reddy, M.M.K., Purohit, H.J., Kapley, A., 2007. Biodegradation of kraft lignin by a newly isolated bacterial strain, *Aneurinibacillus aneurinilyticus* from the sludge of a pulp paper mill. *World J. Microbiol. Biotechnol.* 23, 793–799. <https://doi.org/10.1007/s11274-006-9299-x>.
- Ravi, K., García-Hidalgo, J., Gorwa-Grauslund, M.F., Lidén, G., 2017. Conversion of lignin model compounds by *Pseudomonas putida* KT2440 and isolates from compost. *Appl. Microbiol. Biotechnol.* 101, 5059–5070. <https://doi.org/10.1007/s00253-017-8211-y>.
- Rodrigues, L., Banat, I.M., Teixeira, J., Oliveira, R., 2006. Biosurfactants: potential applications in medicine. *J. Antimicrob. Chemother.* 57, 609–618. <https://doi.org/10.1093/jac/dkl024>.
- Rodriguez, A., Salvachúa, D., Katahira, R., Black, B.A., Cleveland, N.S., Reed, M., Smith, H., Baidoo, E.E.K., Keasling, J.D., Simmons, B.A., Beckham, G.T., Gladden, J. M., 2017. Base-catalyzed depolymerization of solid lignin-rich streams enables microbial conversion. *ACS Sustain. Chem. Eng.* 5, 8171–8180. <https://doi.org/10.1021/acssuschemeng.7b01818>.
- Roy, S., Chandni, S., Das, I., Karthik, L., Kumar, G., Bhaskara Rao, K.V., 2015. Aquatic model for engine oil degradation by rhamnolipid producing *Nocardiopsis VITSISB*. 3 *Biotech* 5, 153–164. <https://doi.org/10.1007/s13205-014-0199-8>.
- Salmela, M., Lehtinen, T., Efimova, E., Santala, S., Santala, V., 2019. Alkane and wax ester production from lignin-related aromatic compounds. *Biotechnol. Bioeng.* 116, 1934–1945. <https://doi.org/10.1002/bit.27005>.
- Sandberg, T.E., Salazar, M.J., Weng, L.L., Palsson, B.O., Adam, M., Diego, S., 2020. Tool for biological discovery and industrial biotechnology. *Metab. Eng.* 56, 1–16. <https://doi.org/10.1016/j.ymben.2019.08.004> (The).
- Sepúlveda, E., Lupas, A.N., 2017. Characterization of the CrbS/R two-component system in *Pseudomonas fluorescens* reveals a new set of genes under its control and a DNA motif required for CrbR-mediated transcriptional activation. *Front. Microbiol.* 8, 1–15. <https://doi.org/10.3389/fmicb.2017.02287>.
- Shi, J., Chen, Y., Liu, X., Li, D., 2021. Rhamnolipid production from waste cooking oil using newly isolated halotolerant *Pseudomonas aeruginosa* M4. *J. Clean. Prod.* 278, 123879. <https://doi.org/10.1016/j.jclepro.2020.123879>.
- Tavares, L.F.D., Silva, P.M., Junqueira, M., Mariano, D.C.O., Nogueira, F.C.S., Domont, G.B., Freire, D.M.G., Neves, B.C., 2013. Characterization of rhamnolipids produced by wild-type and engineered *Burkholderia kururiensis*. *Appl. Microbiol. Biotechnol.* 97, 1909–1921. <https://doi.org/10.1007/s00253-012-4454-9>.
- Teufel, R., Mascaraque, V., Ismail, W., Voss, M., Perera, J., Eisenreich, W., Haehnel, W., Fuchs, G., 2010. Bacterial phenylalanine and phenylacetate catabolic pathway revealed. *Proc. Natl. Acad. Sci. U.S.A.* 107, 14390–14395. <https://doi.org/10.1073/pnas.1005399107>.
- Thorvaldsdóttir, H., Robinson, J.T., Mesirov, J.P., 2013. Integrative Genomics Viewer (IGV): high-performance genomics data visualization and exploration. *Briefings Bioinform.* 14, 178–192. <https://doi.org/10.1093/bib/bbs017>.
- Tiso, T., Narancic, T., Wei, R., Pollet, E., Beagan, N., Schröder, K., Honak, A., Jiang, M., Kenny, S.T., Wierckx, N., Perrin, R., Avérous, L., Zimmermann, W., O'Connor, K., Blank, L.M., 2021. Towards bio-upcycling of polyethylene terephthalate. *Metab. Eng.* 66, 167–178. <https://doi.org/10.1016/j.ymben.2021.03.011>.
- Tiso, T., Thies, S., Müller, M., Tsvetanova, L., Carraresi, L., Bröring, S., Jaeger, K.-E., Blank, L.M., 2017. Rhamnolipids: production, performance, and application. In: Lee, S.Y. (Ed.), *Consequences of Microbial Interactions with Hydrocarbons, Oils, and Lipids: Production of Fuels and Chemicals*. Springer International Publishing, Cham, pp. 1–37. https://doi.org/10.1007/978-3-319-31421-1_388-1.
- Utomo, R.N.C., Li, W.J., Tiso, T., Eberlein, C., Doeker, M., Heipieper, H.J., Jupke, A., Wierckx, N., Blank, L.M., 2020. Defined microbial mixed culture for utilization of polyurethane monomers. *ACS Sustain. Chem. Eng.* 8, 17466–17474. <https://doi.org/10.1021/acssuschemeng.0c06019>.
- van Duuren, J.B.J.H., de Wild, P.J., Starck, S., Bradtmöller, C., Selzer, M., Mehlmann, K., Schneider, R., Kohlstedt, M., Poblete-Castro, I., Stolzenberger, J., Barton, N., Fritz, M., Scholl, S., Venus, J., Wittmann, C., 2020. Limited life cycle and cost assessment for the bioconversion of lignin-derived aromatics into adipic acid. *Biotechnol. Bioeng.* 117, 1381–1393. <https://doi.org/10.1002/bit.27299>.
- Volmer, J., Neumann, C., Bühler, B., Schmid, A., 2014. Engineering of *Pseudomonas taiwanensis* VLB120 for constitutive solvent tolerance and increased specific styrene epoxidation activity. *Appl. Environ. Microbiol.* 80, 6539–6548. <https://doi.org/10.1128/AEM.01940-14>.
- Wang, et al., 2019. Growth of engineered *Pseudomonas putida* KT2440 on glucose, xylose, and arabinose: Hemicellulose hydrolysates and their major sugars as sustainable carbon sources. *GCB Bioenergy* 11 (1). <https://doi.org/10.1111/gcbb.12590>.
- Wei, Y.H., Chou, C.L., Chang, J.S., 2005. Rhamnolipid production by indigenous *Pseudomonas aeruginosa* J4 originating from petrochemical wastewater. *Biochem. Eng. J.* 27, 146–154. <https://doi.org/10.1016/j.bej.2005.08.028>.
- Weimer, A., Kohlstedt, M., Volke, D.C., Nikel, P.I., Wittmann, C., 2020. Industrial biotechnology of *Pseudomonas putida*: advances and prospects. *Appl. Microbiol. Biotechnol.* 104, 7745–7766. <https://doi.org/10.1007/s00253-020-10811-9>.
- Wittgens, A., Santiago-Schuebel, B., Henkel, M., Tiso, T., Blank, L.M., Hausmann, R., Hofmann, D., Wilhelm, S., Jaeger, K.E., Rosenau, F., 2018. Heterologous production of long-chain rhamnolipids from *Burkholderia glumae* in *Pseudomonas putida*—a step forward to tailor-made rhamnolipids. *Appl. Microbiol. Biotechnol.* 102, 1229–1239. <https://doi.org/10.1007/s00253-017-8702-x>.
- Wittgens, A., Tiso, T., Arndt, T.T., Wenk, P., Hemmerich, J., Müller, C., Wichmann, R., Küpper, B., Zwick, M., Wilhelm, S., Hausmann, R., Syldatk6, C., Frank, Rosenau, Blank, Lars M., 2012. Growth independent rhamnolipid production from glucose using the non-pathogenic *Pseudomonas putida* KT2440. *Microb. Cell Factories* 10, 80. <https://doi.org/10.1186/1475-2859-10-80>.
- Wynands, B., 2018. Engineering of *Pseudomonas taiwanensis* VLB120 for the Sustainable Production of Hydroxylated Aromatics.
- Wynands, B., Lenzen, C., Otto, M., Koch, F., Blank, L.M., Wierckx, N., 2018. Metabolic engineering of *Pseudomonas taiwanensis* VLB120 with minimal genomic modifications for high-yield phenol production. *Metab. Eng.* 47, 121–133. <https://doi.org/10.1016/j.ymben.2018.03.011>.
- Wynands, B., Otto, M., Runge, N., Preckel, S., Polen, T., Blank, L.M., Wierckx, N., 2019. Streamlined *Pseudomonas taiwanensis* VLB120 chassis strains with improved bioprocess features. *ACS Synth. Biol.* <https://doi.org/10.1021/acssynbio.9b00108>.

Zhang, R.K., Tan, Y.S., Cui, Y.Z., Xin, X., Liu, Z.H., Li, B.Z., Yuan, Y.J., 2021. Lignin valorization for protocatechuic acid production in engineered *Saccharomyces cerevisiae*. *Green Chem.* 23, 6515–6526. <https://doi.org/10.1039/d1gc01442k>.

Zhu, D., Zhang, P., Xie, C., Zhang, W., Sun, J., Qian, W.-J., Yang, B., 2017. Biodegradation of alkaline lignin by *Bacillus ligniniphilus* L1. *Biotechnol. Biofuels* 10, 44. <https://doi.org/10.1186/s13068-017-0735-y>.

Zobel, S., Benedetti, I., Eisenbach, L., De Lorenzo, V., Wierckx, N., Blank, L.M., 2015. Tn7-Based device for calibrated heterologous gene expression in *Pseudomonas putida*. *ACS Synth. Biol.* 4, 1341–1351. <https://doi.org/10.1021/acssynbio.5b00058>.